

03

The Backscattering Polarization for a Sphere with a Two-Scale Relief of Rough Surface

© E.V. Klass, S.A. Ulyanov, I.Y. Belorybkin

D.Mendelev Central Research and Development Institute of Chemistry and Mechanics („TsNIIHM“),
115487 Moscow, Russia

e-mail: elenaklass@yandex.ru

Received July 7, 2022

Revised August 22, 2022

Accepted September 09, 2022

The paper presents the results of studies of the polarization of backscattered optical radiation for a model of a sphere with a wavy surface covered with arbitrarily oriented ellipsoidal pores. The calculations were performed by the Monte Carlo method (ROKS-RG program, geometrical optics approximation). Surface roughness of objects is taken into account using local geometries. It is shown that for structures whose pores contain a vitreous medium, the presence of vacuum voids between a transparent and opaque medium determines the nature of the phase dependence of the degree of polarization. In the absence of vacuum, the polarization is always positive and, for small phase angles, depends significantly on the optical characteristics of an opaque medium. The presence of vacuum is a catalyst for the growth of the p-component of the reflected radiation. This leads to a significant decrease in the amplitude of the positive polarization branch. Differences in the optical characteristics of opaque materials are also leveled out, and in some cases negative values of the degree of polarization are observed in the region of small phase angles.

Keywords: polarization, geometrical optics approximation, Monte Carlo method, rough surface, Two-Scale Relief.

DOI: 10.21883/EOS.2022.11.55101.3904-22

Introduction

Studies of various characteristics of reflected optical radiation from heterogeneous and rough surfaces in many cases aid to draw conclusion about the surface structure, shape and material of the object. For example, the high sensitivity of the polarization characteristics of the reflected radiation to the degree of roughness made it possible to develop an optical method such as ellipsometry [1], which is based on the analysis of amplitude and phase changes during the interaction of polarized optical radiation with the reflecting surface of the study object. The mathematical apparatus of ellipsometry, based on the Drude approximation and recurrence relations using Fresnel formulas, is focused on researching of thin films, as well as thin-film systems produced on the basis of semiconductor and dielectric materials [2,3]. To date, ellipsometry has been widely used in practice to assess the quality control of surfaces formed both in the production of nanoscale structures and for machine parts, the surface of which is subjected to grinding [4]. Monte Carlo methods [5] are also involved in simulating the polarization of the reflected radiation of a rough surface with arbitrary number of layers and profiles.

In ellipsometry, the concept of direct and inverse problems is widely used. In the first case, polarization characteristics are determined from the known internal parameters of the structure (optical constants, layer thicknesses etc.), in the second case, the parameters of the surface structure are determined from the known polarization characteristics. The solution of the inverse problem is almost always carried

out by numerical methods, and the solution itself is often ambiguous.

A vivid example of attempts to find a solution to the inverse problem in a somewhat different branch of optical science is the problem of estimating the structure of the reflecting surface of atmosphereless bodies of the Solar System based on the known polarization and amplitude characteristics of backscattered optical radiation.

These bodies are constantly exposed to energetic-particle streams and bombarded by meteor particles that vary in shape, size and energy. As a result, a fairly complex multiscale relief with a large number of craters is formed on the surface. Due to the absence of an atmosphere, the orientation of the craters can be arbitrary. The surface of the craters, in turn, is covered with the so-called regolith, i.e., uncemented products of disruption & redeposition of rocks. This material consists of rock fragments, meteorite particles, and products of multiple collisions of meteor particles that melted, crushed, and mixed the surface material. Particle size is from fractions of a millimeter to tens of centimeters in diameter [6].

Solar radiation reflected from the surface of atmosphereless bodies has several features. The main ones include a significant decrease in the dependence of the back reflection indicatrix in the region of small phase angles and the presence of a negative branch in the dependence of the degree of linear polarization of the reflected radiation also in the region of small phase angles [7]. The phase angle is defined as the angle between the direction from the source (the Sun) to the reflecting body and from the

reflecting body to the detector (observer). The degree of polarization of reflected radiation is understood as the value calculated by the relation $P = (F_{\perp} - F_{\parallel}) / (F_{\perp} + F_{\parallel})$, where F_{\perp} , F_{\parallel} are components of optical radiation reflected from the object in a plane perpendicular (s) and parallel (p) to the plane of incidence, respectively. As an example, it should be pointed out that for such an atmosphereless body as the Moon, the decrease of the indicatrix is ~ 1.6 times for phase angles up to 10° , while negative polarization is observed for angles in the range $0-23.5^{\circ}$ and $\sim 1\%$ at the minimum. It should be noted that these features are characteristic of any region on the Moon's surface.

A recent work [8] points out that, despite careful study with ground-based telescopes, telescopes in Earth orbit, remote sensing telescopes in deep space, and laboratory analyzes of the phase curves of reflectance and polarization, at present there is no generally accepted single physical mechanism that would explain both the phenomena of reflection and polarization. In a detailed review of this work on the current state of research, it is noted that the results obtained in recent decades show that the opposition effect and polarization effects can arise as a result of different processes and depend on the albedo and particle size of the studied materials.

From the point of view of explaining the mechanisms of polarization of atmosphereless bodies, detailed critical analyzes of model and, especially, its negative branch, presented in the monograph [9], as well as in the review article [10], are rather relevant. In particular, the works [11,12] are noted, where it is shown that the negative polarization for small phase angles can be due to scattering by a single particle, although the mechanism of its formation is not obvious in this case. It is suggested that negative polarization can be associated with wave effects for particles of light, for example, with the so-called near-field effects [13] or coherent backscattering, which occurs for a group of particles smaller than the wavelength when the rays, transmitting in opposite directions interfere with each other [14-16]. It should be noted that in most models the particle shape was assumed to be spherical.

In recent years, several articles have appeared in which, for predicting the polarization features of the reflected radiation of comets, which are dust clots, a model using agglomerated particles of irregular shape and various chemical compositions of several micrometers in size has proved itself quite successfully [17,18]. In this case, as the authors point out, the mixture of particles should contain particles from a weakly absorbing material (for example, water ice).

It is noted in the work [19] that one of the shortcomings of currently used methodologies is that they can only be applied in a limited range of particle sizes; mainly for particle sizes comparable to the wavelength. Numerical methods such as the discrete dipole approximation (DDA) and finite difference time domain (FDTD) [20,21] algorithms require a significant increase in computational resources as particle size increases with respect to wavelength, which is currently limits the maximum practical particle size. The authors

of [19] supplemented the coherent scattering model by the Monte Carlo ray tracing mechanism and used it to calculate clusters of spherical particles with sizes much larger than the wavelength. The development of models using ray tracing for particles exceeding the wavelength was continued in [22], and in [23] the multiscale light scattering model is presented, in which, for different scales for size dimension of the target (nano-, micro- and millimeter-scales) various simulating tools are used.

The work [24] is devoted to attempts to create a unified physical mechanism and evaluate the structure of reflecting surface on the basis of both polarization and amplitude characteristics of backscattered radiation. The authors used the far-field approximation model (the scattering medium consists of clusters located in each other's far zones) in calculations of coherent near-field backscattering, i.e., for a close-packed weakly absorbing medium, and obtained fairly good agreement with some laboratory data.

It should be noted that a significantly larger number of works are devoted to estimates of the structure of a reflecting surface based on studies of amplitude characteristics than on the basis of polarization characteristics. Thus, for example, in the work [25] the effect of different types of topographies on the back reflection indicatrix, the characteristic scale of which is much larger than the surface size of particle, was studied. The calculations were carried out within the framework of the geometrical optics approximation based on ray tracing by the Monte Carlo method. It was not possible to obtain the desired dependence of the reflection indicatrix, but it was shown that rocky topographies produced by randomly distributed stones on a flat surface show much steeper phase curves than a surface with random topography obtained based on Gaussian statistics of height and slope distributions.

Peculiarities of reflection from pores of ellipsoidal type for single-scale geometry are clearly presented at a qualitative level in [7], p. 209, Fig. 16. The main objection of the author of [7] against the use of this model was that for vertical viewing angles the steep dependence of the back reflection can be explained, but this one cannot be explained for large angles.

In [26,27] the results of studies on the formation of the reflection indicatrix for a sphere with a two-scale rough surface relief were presented and it was shown that for a sphere relief in the form of undulant surface covered with arbitrarily oriented ellipsoidal pores, varying the roughness parameters makes it possible to obtain the phase dependence of the inverse reflection close to the phase dependence of the Moon. Ray tracing by the Monte Carlo method and geometric optics approximation were used as a tools.

Present work is in some way a continuation of [27] and is devoted to study on the formation of the polarization of backscattered radiation in the framework of a two-scale model of a sphere containing ellipsoidal pores.

Methodology of calculation and object under study

To calculate the reflected optical radiation, a mathematical apparatus is used, which, when solving the equation for the transfer of light radiation in a three-dimensional setting, uses the Monte Carlo method. The theory of radiative transfer as applied to optical radiation considers the process of radiation propagation as a transfer of particles, the photons. At that the wave effects of reflection and refraction at the interfaces between different media are taken into account with the help of special boundary conditions.

The standard stationary equation for the transfer of polarized radiation in a scattering medium in the integro-differential form is written as

$$(\omega, \text{grad} I(r, \omega)) = -\sigma_t(r, \omega)I(r, \omega) + \int_{\Omega} \sigma_s(r, \omega')I(r, \omega') \times g(\omega', \omega, r)d\omega' + I_0(r, \omega),$$

where $I(r, \omega)$ is vector function (Stokes vector) of radiation intensity at point r in ω direction, I_0 is vector function of particle source distribution density, σ_t is total radiation interaction cross section at a point r in the ω direction, including the scattering cross section σ_s and the absorption cross section σ_a ($\sigma_t = \sigma_s + \sigma_a$), $g(\omega', \omega, r)$ is matrix function of the scattering of a photon that changes the direction of motion ω' to the direction ω . The components of the Stokes vector $I(r, \omega)$ are determined by the radiation intensity and polarization parameters (polarization plane, degree of ellipticity etc.).

We are solving the problem of determining the reflection of polarized radiation from an opaque three-dimensional object G with a rough surface S . In this case, part of the surface may contain regions covered with transparent materials of finite thickness d . Let the object G of interest to us have regions i that are homogeneous in terms of physical properties. Let us introduce into consideration the surfaces S_{i-} and S_{i+} , which describe the inner and outer interfaces S_i of homogeneous regions G_i . The boundary conditions on these surfaces can be written as

$$I(r, \omega)|_{S_{i-}} = \hat{F}(r, \omega)I(r, \omega)|_{S_{i+}} = \hat{R}(r, \omega)I(r, \omega)|_{S_{i+}} + \hat{T}(r, \omega)I(r, \omega)|_{S_{i+}},$$

where the operators \hat{F} , \hat{R} and \hat{T} describe the optical properties of materials in the form of reflection and refraction coefficients, respectively, obtained on the basis of Fresnel formulas [9].

Taking into account the fact that in our case the medium is not scattering ($\sigma_s = 0$), but a transparent material can have an absorption cross section σ_a different from zero, the transfer equation takes the form

$$(\omega, \text{grad} I(r, \omega)) = -\sigma_a(r, \omega)I(r, \omega) + I_0(r, \omega).$$

To estimate the desired reflection indicatrix as a linear functional of the form

$$I(\omega) = \int_S I(r, \omega)dr,$$

where the integration is carried out over the surface S of the region G , the solution of the equation can be represented as a Neumann series in terms of the number of intersections [28] by a photon of the interface between different media. Between the points of intersection of the interfaces in the medium, the photon flux propagates along the characteristic. When crossing interfaces, the transformation of the Stokes vector is carried out according to the rules of matrix optics $I' = FI$, where F is the Fresnel reflection matrix. So, for example, when simulating the reflection from a rough surface, the Stokes vector of the reflected radiation that has experienced n reflections will be written in the form $I' = R_n F_n, \dots, F_2 R_1 F_1$, where F_n is the Fresnel matrix for the n th reflection, R_n is the rotation matrix of the reflection plane when the ray passes from the $(n-1)$ th to the n th area element. The angle of rotation is determined by the directions of the normals to the specified area elements, and the formula for the rotation matrix can be found in [29,30].

The simulation of optical radiation transfer processes was carried out using the ROKS-RG [31] program, which was developed to evaluate the characteristics of optical radiation fields in three-dimensional objects with a rough surface by the Monte Carlo method in the geometrical optics approximation. The geometric module of the program is focused on the representation for object in the form of combination of geometric zones bounded by second-order surfaces. The control of the correctness for the calculation geometry specification is carried out using a specially developed original visualization algorithm [32].

The physics of the interaction of optical radiation with materials, implemented in the program, includes the processes of reflection and refraction, the probability of which is determined on the basis of the Fresnel formulas, as well as the processes of diffuse reflection. The complex refractive index $m = n + ik$ is used as the initial parameter when calculating the probabilities of reflection and refraction, on the basis of which the ratios of energy flows are calculated, each of which, in turn, is proportional to the square of the corresponding amplitude. Formulas for calculating the probabilities of reflection and refraction for s - and p -polarized radiation in the case of a complex refraction index can be found, for example, in [9].

In transparent media with absorption coefficient k that is not equal to zero, the absorption of radiation is estimated exponentially in accordance with the Bouguer–Lambert law, in which the absorption coefficient per unit length α is calculated in accordance with the formula $\alpha = 4\pi k/\lambda$, where λ is wavelength. The value of the path of a photon in a transparent medium is determined on the basis of

the coordinates of the particle trajectory when successively crossing the boundaries of the specified medium.

The approximation of geometric optics makes it possible to use the similarity law when specifying the dimensions of the computational scheme of an object. Namely, the results of calculations obtained in three-dimensional geometry with linear dimensions XYZ can be extended to geometry with dimensions $\alpha(XYZ)$, where α is proportionality coefficient. Based on this, an approach was implemented in the program that allows one to evaluate the reflection properties of a three-dimensional object with a rough surface.

The essence of the approach lies in the representation of the geometric description of the object at two levels: as a whole the description is set at macrolevel, and the roughness is set at the microlevel. Similar idea was originally proposed in the work [33], where the microlevel geometry was formed as a random tetrahedral „well“. But in this case it is impossible to take into account the multiple reflection associated with the transfer of radiation between neighboring „wells“. In [31] it was proposed to specify the microlevel geometry intended for describing roughness in the form of a rotation body population placed on the substrate. Ellipsoids, cones, paraboloids, hyperboloids, etc., were considered as such. Required degree of roughness is simulated by the shape and parameters of the figures, in particular, their height and radius. Such a representation of microgeometry makes it possible to correctly take into account the effects of multiple reflections of a rough surface. For the object with multiscale surface relief, several successive microlevels can be used. It should be noted that the similarity law makes it possible to use relative units not only for the macrolevel, but for the microlevels when identifying linear dimensions.

The simulating of optical quanta trajectories starts at the first level (macro), which is considered to be the highest. When a particle hits the surface of a macrogeometry marked as rough one, a transition to the microlevel occurs, i.e., the particle coordinates are recalculated from the main geometry to the local one. In this case, the program remembers the direction cosines, particle coordinates, and the number of the equation that determines the transition surface to the geometry of the given level. When calculating the coordinates and direction vectors of particle in the local system, it is assumed that its Z axis is directed (depending on the problem) either along the normal to the surface, which determines the zone of transition to the local system, or is played out uniformly with respect to the specified normal. The remaining directions are determined by formulas that describe the rotation of the old coordinate system relative to the new one by the corresponding angle.

At the microlevel, the trajectory of a particle is traced until it leaves microlevel's limits. In this case, in each act of interaction of a particle with inhomogeneities of microgeometry, a mirror reflection is played out, and the weight of the reflected particle is calculated using the Fresnel formulas for the corresponding material. Then the return to

the macrolevel is made and the simulating of the trajectory in macrogeometry continues.

The limitations of the proposed algorithm lie in the fact that when organizing a successive return of a particle from microgeometries to macrogeometry, it is assumed that it has the same coordinates that it had before the transition to the microgeometry of the previous level, i.e. roughness only changes the direction of particle movement, not its coordinates. It follows from this limitation that the proposed approach is correct for opaque materials. However, transparent materials can also be used in multiscale geometries if the above limitations can be accepted for the structure under study. Transparent materials that have absorption coefficient that is not equal to zero attenuate radiation non-linearly. Therefore, the similarity law does not apply to them, and their use for simulating the reflection of optical radiation in multiscale geometry is incorrect.

Let's also indicate here several features for the organization of standard particle simulation by the Monte Carlo method. The radiation source is usually represented as a wide monodirectional beam of particles. The playing out of the initial coordinates of the particle is performed on the outer surface of the object, uniformly over the projection area on the direction of incidence of radiation. When simulating a trajectory, each particle is assigned the initial weight. When a particle crosses the surface of the object under study, the surface material is determined for the intersection point, and for this material, in accordance with the given probabilities, the type of reflection (mirror or diffuse) is played out. For the selected reflection process, the direction of reflection is determined by the corresponding formulas and the weight of the particle is corrected. When a particle enters the detection zone, its trajectory is interrupted, and the weight gained on the trajectory is fixed. The P sphere, which includes the calculated object, can be taken as the reflected radiation registration zone. The weight of the escaped particle, in accordance with the direction of its motion, is fixed on an angular grid, which divides all possible directions in polar and azimuth angles into separate cells. To register radiation, it is convenient to use the Carlson grid [34], in which the number of partitions in the azimuth angle depends on the cosine of the polar angle, which allows one to partition the sphere of solid angles into cells of equal area.

In our case, the object under study was a sphere, the geometric description of the roughness of which included two blocks of microgeometries. One of them simulated an undulant surface, for which the population of halves of ellipsoids was used, and the second modeled a porous surface, for which ellipsoids were also used.

Testing the methodology

The results of verification of the ROKS-RG program on the data of numerical analytical calculations for geometries with smooth surfaces and experimental studies for reflection

from randomly rough surfaces and a three-dimensional object are presented in [31]. Testing of the program as applied to a porous surface is presented in [26] based on a comparison with the results of the experiment in which the attenuation of optical radiation in cone-shaped pores formed during etching of a nickel plate was studied. When verifying the program in application to the calculation of back reflection for geometries with a two-scale surface relief, [27] showed satisfactory agreement with the results of the experiment, in which several variants of a two-scale rough surface were prepared and back reflection was measured for s -components of s -polarized radiation.

According to the Fresnel formulas, the reflected radiation for opaque bodies always has a non-negative degree of polarization. Since we are interested in the possibility of forming a negative polarization, then transparent media must be present in the structures under study.

For the sake of presented work, the program was tested on the results of several studies of previous years obtained by different authors for the degree of polarization of transparent media (Fig. 1). Fig. 1, *a* shows a comparison with the calculations of a transparent sphere from [35] with $m = 1.55 + 0i$, where the geometrical optics approximation works in its pure form and the size of the sphere is unimportant. Fig. 1, *b* presents a comparison with the results from [36], obtained in the experiment from the PROGRA² series, as well as with calculations by the Mie theory for a single sphere with radius $50\ \mu\text{m}$ made of diamond with $m = 1.51 + 0.00085i$ and $\lambda = 632.8\ \text{nm}$. Experiments of the PROGRA² series were developed to measure the degree of polarization of particles of various compositions on the unit simulating microgravity conditions.

In both considered cases, there is a satisfactory agreement between the compared data.

Calculation result

Recall that the main object under study was a sphere, the geometric description of which included two blocks of microgeometries. One of them simulated an undulant surface, for which the population of halves of ellipsoids was used, and the second modeled a porous surface, for which ellipsoids were also used. The sphere was irradiated by a unidirectional particles flux. When conducting research, we simulate a situation where the source and detector are at considerable distance from the object, which is much larger than the size of the object. Therefore, the calculation results are presented as a dependence of the reflecting characteristics on the source-sphere-detector angle, which in what follows will be called as the phase angle.

Sphere of opaque materials

At the first stage of research, the coating of the sphere was assumed to be opaque. The polarization calculations were carried out for materials with different complex

refraction indices in the region of 550 nm wavelengths, on the basis of which the values of the reflection coefficient ρ were calculated. Spheres were considered, the surface of which has single-level roughness in the form of convex halves of ellipsoids and two-level roughness i.e. in the form of undulant surface with ellipsoidal arbitrarily oriented pores.

To denote the degree of inhomogeneity of a rough surface simulated using convex elements, by analogy with [27], let's will use the value of the ratio σ/τ , where σ is standard deviation heights of inhomogeneities, and τ is correlation length. The roughness of the porous surface will be characterized by the value of the aspect ratio sa , characterized by the ratio of the pore depth d to its radius $r-d/r$.

The calculations performed showed that for a two-scale sphere, the degree of polarization is mainly affected by the geometry of the lower level, which describes the porous surface. The position of the maximum in all cases approximately corresponds to the double Brewster angle, and the amplitude of the maximum has an inverse relationship with respect to the reflectivity of the material. Studies have also shown that as the pore depth increases, the position of the maximum shifts to the region of smaller angles, and maximum's amplitude decreases. It is interesting to note that for very deep pores at $sa \sim 3$ and above, the curve of the degree of polarization flattens out.

As an example, Figures 2, *a* and 2, *b* show some results of calculating the phase dependence of the degree of polarization P of radiation for a sphere with one-level and two-level roughnesses made of materials with different reflection coefficients ρ .

Single pores containing vitreous medium

The second stage of research was devoted to studying the formation of the polarization degree of a single pore, inside which there is a vitreous material. The pore filling had a layered structure: first a vacuum, then a vitreous material, followed by an opaque one. The possibility of the presence of vacuum voids between the vitreous and opaque materials, simulating a loose fit of the vitreous material to the main opaque medium, was also considered. Let us denote by the value h the thickness of the glassy material along the axis of the pore, and h_1 denote the thickness of the vacuum (if any). The pore depth d in this case refers to the distance from the pore surface to the vitreous medium.

Irradiation was simulated as a parallel particle beam directed along the pore axis. The polarization degree was calculated depending on the angle of radiation reflection. The optical constants for the vitreous material were chosen to be $m = 1.6 + 0.00001i$.

The calculation results showed the following.

For small pores with parameters $r \gg d$, the polarization degree at small reflection angles is close to zero, and a change in the thickness of the transparent material has little effect on the polarization degree. As the pore depth increases, differences appear in the dependence of the polarization

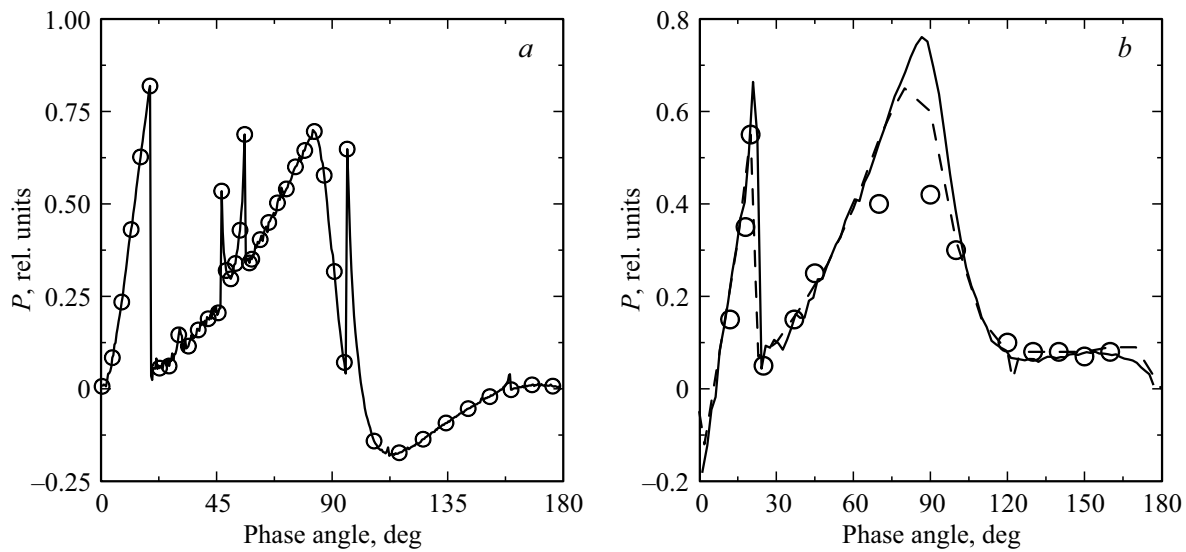


Figure 1. (a) Dependence of the degree of polarization on the phase angle for a sphere with $m = 1.55 + 0i$. Solid curve — ROKS-RG, \circ — [35]. (b) Dependence of the degree of polarization for a sphere ($r = 50 \mu\text{m}$) made of diamond ($m = 1.51 + 0.00085i$). \circ — experiment [36], dashes — Mie theory [36], solid curve — ROKS-RG.

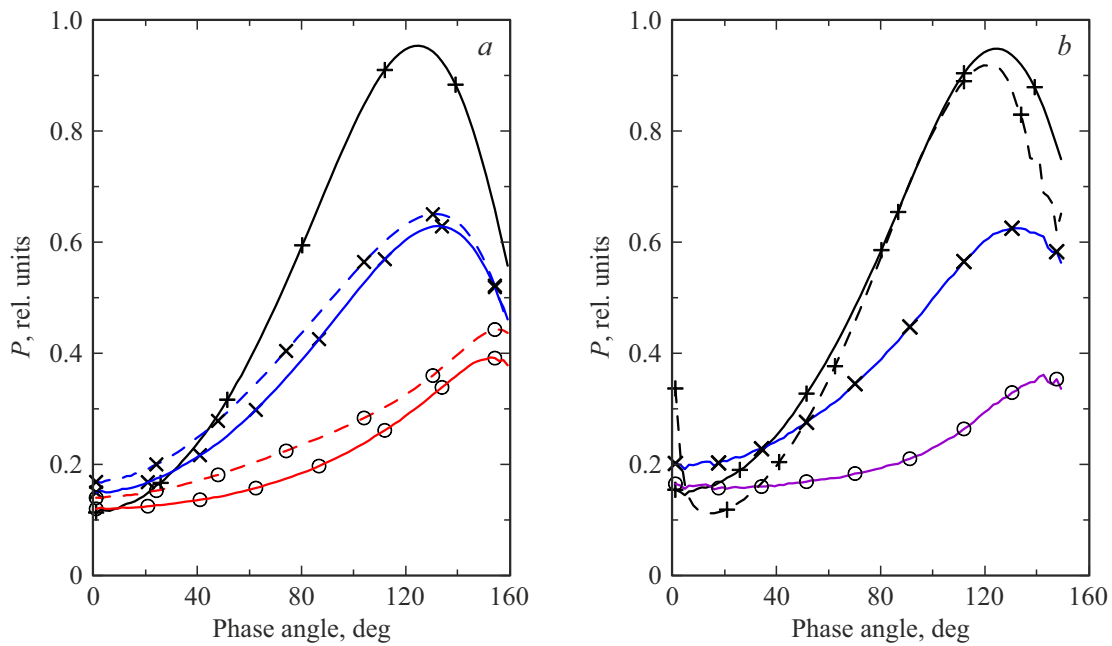


Figure 2. Polarization degree of the sphere for opaque materials with different ρ : 0.11(+), 0.33(x), 0.7(o). Single-level roughnesses (a): solid curve — $\sigma/\tau \sim 0.38$, dashes — $\sigma/\tau \sim 0.06$; two-level roughnesses (b): first level $\sigma/\tau = 0.38$, second level — pores: solid curve — $d/r \sim 0.5$, dashes — $d/r \sim 1.5$.

degree on the presence or absence of vacuum voids between transparent and opaque materials and on the thickness of the transparent material h . As an example, Figs 3,4 show the corresponding dependences for a pore with $d/r \sim 0.5$ and $d/r \sim 1.5$, respectively. Fig. 3 demonstrates that in the absence of vacuum (dashes) for the same thickness h , the polarization degree is always positive and depends on

the reflection coefficient of the opaque material. And if it is present (solid curve), the polarization degree at small values of the reflection angle can be negative and weakly depends on the reflection coefficient of the opaque base. Figure 4 shows that for the same opaque material in the absence of vacuum (dashes) the polarization is always positive and weakly depends on the thickness h . In this case, at small

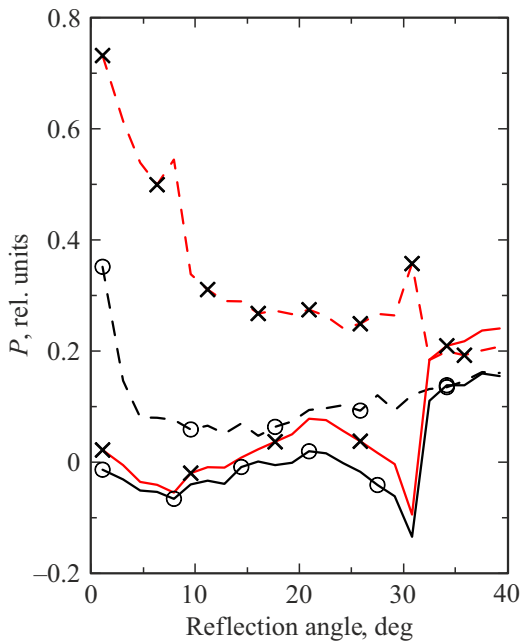


Figure 3. Influence of the material on the polarization of the reflected radiation of a single pore. Reflection coefficient ρ : 0.11(\circ), 0.33(\times). Solid curve — with vacuum, dashes — without vacuum. \circ — $h \ll r$, \times — $h \sim r$.

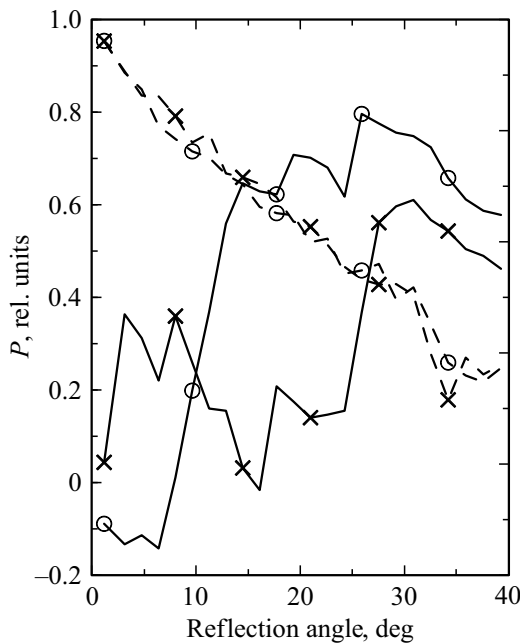


Figure 4. Influence of the thickness h of vitreous medium on the polarization degree for a single pore with $d/r = 1.5$. Solid curve — with vacuum, dashes — without vacuum. \circ — $h \ll r$, \times — $h \sim r$.

reflection angles, the polarization degree is close to unity; as the reflection angle increases, its values decrease. In the presence of a vacuum (solid curve), the polarization depends on the thickness of the transparent material h , and

therewith has an irregular character, and its value for some ranges of reflection angles can be negative.

Studies on the effect of the absorption coefficient of vitreous material on the polarization degree also showed a difference in the behavior of the dependences on the presence or absence of vacuum voids. In the absence of vacuum, the absorption coefficient does not affect the polarization, and in presence of vacuum, the polarization degree increases with increase in the absorption coefficient.

The physical mechanism that determines the behavior of phase dependences in the presence of vacuum voids is associated with total internal reflection at the interface between the vitreous medium and vacuum. Initially, in a vitreous medium, according to the Fresnel formulas, the p -component of the refracted radiation is greater than or equal to the s -component. Further, when passing from an optically denser medium (vitreous medium) to an optically less dense medium (vacuum), starting from a certain angle of incidence $\theta_{in} \sim \arcsin(1/n)$, total reflection of light occurs. The quanta incident on the interface at angles from 0 to θ_{in} are partly reflected and partly refracted in the usual way. For angles greater than θ_{in} , the s - and p -components are reflected equally, i.e., if more p -polarized radiation has passed into a transparent medium, then more of it will be reflected. Refracted quanta from a limited range of incidence angles fall on an opaque material that follows vacuum (thereby further reducing their total number), which have a negative degree of polarization. Studies have shown that further reflection of quanta from opaque material increases the number of s -polarized quanta, but the previous decrease in the total number of quanta falling on opaque material leads to the fact that their contribution to the total sum of the s -component of the reflected radiation is sufficient small.

Fig. 5 shows the results of calculations of the contributions to the angular distribution of the reflected radiation flux from quanta that were reflected from an opaque material (solid curve, $\rho = 0.33$) and quanta that did not reach it and were reflected from a transparent material (dashes), for cases where there is no vacuum between transparent and opaque materials and when it exists. It can be seen from Fig. 5, a that in the absence of vacuum, the contribution of the s -component for quanta that are reflected from opaque medium can be higher than when reflected from transparent medium. In both cases, the contribution of the p -component is much smaller. In the presence of vacuum (Fig. 5, b), the contributions of the s - and p -components reflected from the first medium are close to each other at small reflection angles, and sometimes the value for p -component exceeds the value of the s -component. The contribution from the second, opaque medium is generally several times lower than the contribution from the first medium. It can be said that vacuum acts as a catalyst for the increasing of the p component of the reflected radiation.

It is worth pointing out that if the linear dimensions of the vacuum cavity are of the order of a wavelength or less, the manifestation of the effect of attenuated total internal

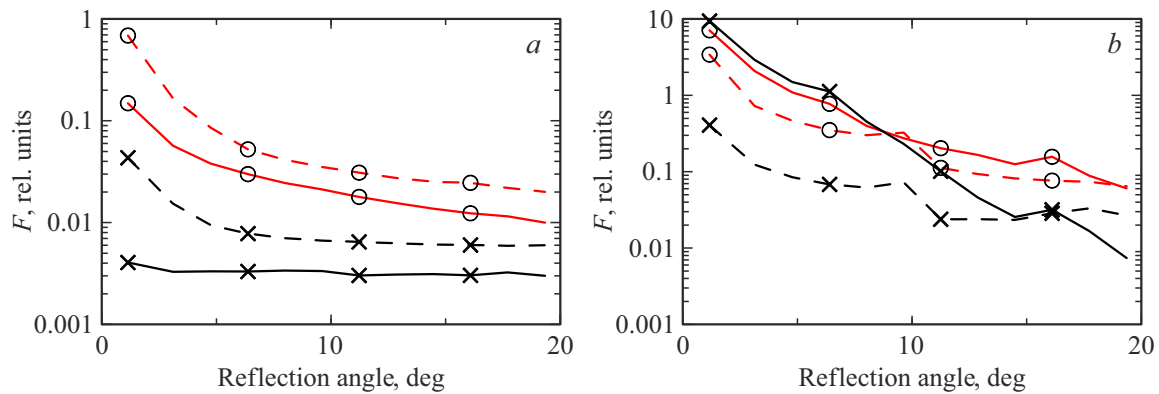


Figure 5. The contribution of the s (\circ) and p (\times) components upon reflection from a transparent (solid curve) medium and opaque (dashed curve) medium in the absence of vacuum (a) and in the presence of vacuum (b).

reflection (ATIR) is possible, in which ellipsoidal or circular polarization of radiation occurs [37,38]. But consideration of this effect related to wave optics is beyond the scope of this work.

Two-scale sphere with pores containing transparent material

As mentioned above, the calculations were carried out for a sphere with a two-scale surface relief: the undulant surface is covered with arbitrarily oriented pores, the geometry of which has a layered structure: vacuum, vitreous material, and an opaque base. Variants were also considered, in which the presence of a vacuum between the vitreous and opaque materials was provided. Absorption in the vitreous material was not taken into account.

Studies have shown that the main influence on the degree of polarization of a two-scale sphere is exerted by the geometry of the lower level, which describes the porous surface.

Studies have also shown that the degree of polarization of a two-scale sphere in the presence of a vacuum cavity inside ellipsoidal pores largely depends on the depth of the pores and the thickness of the transparent material. Examples of the dependence of polarization degree on the pore depth for the same thickness of the transparent material are shown in Fig. 6, and on the thickness of the transparent medium for the same pore depth are shown- in Fig. 7.

An analysis of the calculation results showed that for pores with a depth of $0.7 \leq d/r \leq 1.3$ and for a sufficiently large thickness of the transparent material $h > d$, the degree of polarization has negative values in the region of small phase angles. For deeper pores, the negative branch of polarization is absent, and as the pore depth increases, the value of P at zero increases. The position of the maximum for the positive polarization branch and its amplitude are also determined by the pore depth. For pores with $d/r \leq 1$, the maximum is observed in the range of angles $110-130^\circ$. With increase in the pore depth, its position shifts to the range of angles with smaller values with a simultaneous

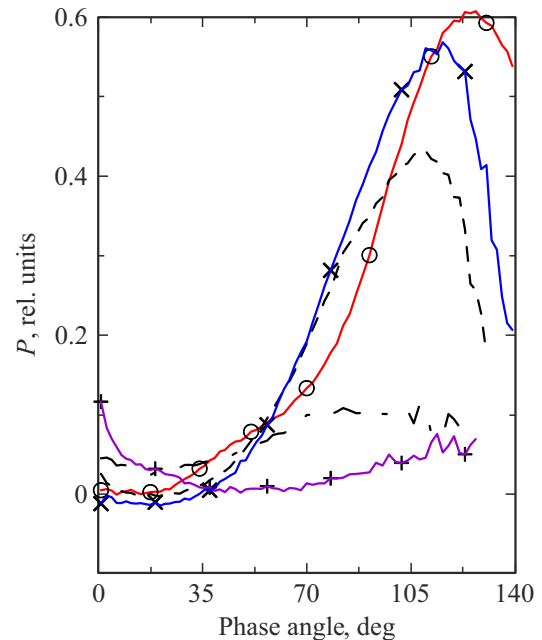


Figure 6. The polarization degree of reflected radiation for a two-scale sphere ($\sigma/\tau \sim 0.38, h > d$ for pores of different depths d/r : 0.2 (\circ), 1.0 (\times), 1.2 (dashes), 1.8 (dash-dotted lines), 3.0 ($+$).

decrease in the amplitude. Change in the thickness of transparent material at the same pore depth ambiguously changes the nature of the dependence of polarization degree on the phase angle (Fig. 7).

Fig. 8 shows the influence of the presence of a vacuum cavity between a transparent and opaque medium on the degree of polarization for materials with different values of the reflection coefficient of an opaque base. The data are presented for the relief with pore parameters $d/r \sim 1$ (Fig. 8, a) and $d/r \sim 1.5$ (Fig. 8, b). It is clearly seen that in the absence of vacuum, the maximum in the positive polarization branch is close to 1, while in the presence of vacuum, the amplitude of the maximum is much smaller. And the greater the pore depth, the more significant the

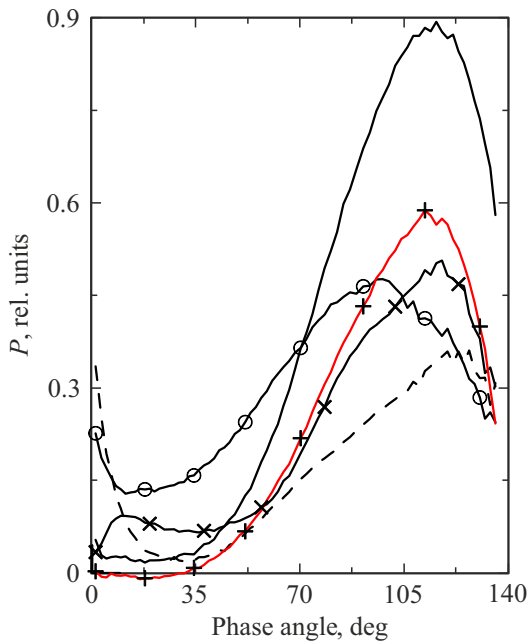


Figure 7. The polarization degree of reflected radiation by a two-scale sphere ($\sigma/\tau \sim 0.38$, $d/r \sim 1$) for different thicknesses of a transparent medium h/r : 0.1 (\circ), 0.8 (dashes), 1.2 (\times), 3.0 ($+$), 8.0 (solid curve).

decrease in amplitude. For instance, for pores with a depth of $d/r \sim 1$, the amplitude of the maximum decreases by a factor of 2, and for pores with a $d/r \sim 1.5$ decreases by a factor of 4. Another feature is that the polarization curve in the presence of vacuum practically does not depend on the optical characteristics of opaque materials in the entire

range of phase angles, i.e., the presence of vacuum levels out their differences. And in the absence of vacuum, significant differences are observed in the degree of polarization with a change in the optical characteristics of an opaque base. These differences are especially noticeable in the range of phase angles up to $\sim 60^\circ$.

Conclusion

The calculation of the polarization degree was carried out in the work in the approximation of geometrical optics for an idealized model, which is quite far from real structures found in nature. Nevertheless, the presented results make it possible to evaluate the influence of various factors on the formation of the polarization characteristics of reflected optical radiation in structures containing a vitreous medium in ellipsoidal pores. One of these factors is the presence of vacuum voids between vitreous and opaque media. In the absence of vacuum, the degree of polarization is largely determined by the optical characteristics of the opaque medium. The presence of vacuum voids is a catalyst for the increase of the p component of the reflected radiation, due to which the amplitude of the positive branch of the degree of polarization is significantly reduced compared to structures in which voids are absent, and in some cases, in the region of small phase angles, its value takes on negative values. In this case, the differences in the optical characteristics of opaque materials are leveled out, i.e., the degree of polarization is practically independent of them.

The results obtained may be useful in the development of models for explaining the phenomena associated with

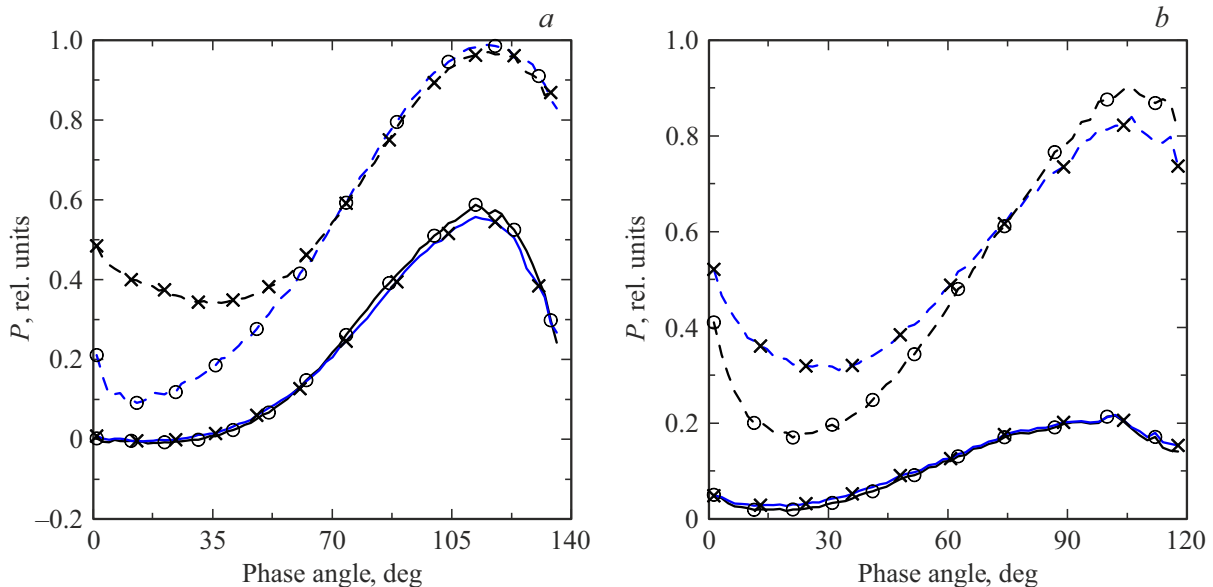


Figure 8. Influence of the vacuum cavity on the degree of polarization for a two-scale sphere. (a) $\sigma/\tau \sim 0.38$, $d/r \sim 1$, $h \sim 3d$; (b) $\sigma/\tau \sim 0.38$, $d/r \sim 1.5$, $h \sim 2d$. Solid curve — with vacuum, dashes — without vacuum. The reflection coefficient of the opaque material is $\rho = 0.11$ (\circ), 0.33 (\times).

the reflection and polarization of non-atmospheric bodies, as well as in other practical applications.

Conflict of interest

The authors declare that they have no conflict of interest.

References

- [1] V.K. Gromov. *Vvedeniye v ellipsometriyu* (Ed. Leningrad State University, L., 1986), 191 p. (in Russian)
- [2] K.G. Sekarin. *Study of the physical and technical characteristics of inhomogeneous media by polarization-optical methods*. Extended abstract of the thesis for cand. dis. (St. Petersburg State University ITMO, St. Petersburg, 2009) (in Russian).
- [3] S.N. Svitashcheva. *Ellipsometriya sherokhovatykh poverkhnostey*. Extended abstract of the thesis for cand. dis. (Institute of Physical Problems of SB RAS, Novosibirsk, 2009) (in Russian).
- [4] R.R. Ziyatdinov, A.A. Shabaev, R.R. Valiakmetov. *Fund.Issl.*, **12**, 287 (2017) (in Russian).
- [5] Chi Wang, Jun Gao, Tingting Yao, Lingmei Wang, Yongxuan Sun, Zhao Xie, Zhongyi Guo. *Opt. Soc. of Am.*, **24** (9), 9397 (2016).
- [6] A.V. Mokhov, P.M. Kartashov, T.A. Gornostaeva, A.P. Rybchuk, O.A. Bogatkov. *Kristallogr.*, **66** (4), 610 (2021) (in Russian).
- [7] *Fizika i astronomiya Luny*, ed/ by Z. Kopal (Mir, M., 1973), ch. 5 (in Russian).
- [8] R.M. Nelson, M. Boryta, B.W. Hapke, K. Manatt, Yu. Shkuratov, V. Psarev, K. Vandervoort, D. Kroner, A. Nebedum, Chr.L. Vides, J. Quiñones. *Icarus*, **302**, 483 (2018).
- [9] Br. Hapke. *Theory of reflectance and emittance spectroscopy* (Cambridge University Press., 1993).
- [10] Y. Shkuratov, V. Kaydash, V. Korokhin, Y. Velikodsky, N. Opanasenko, G. Videen. *Planet. and Space Sci.*, **59**, 1326 (2011).
- [11] Y. Shkuratov, A. Ovcharenko, E. Zubko, H. Volten, O. Munos, G. Videen. *J. Quant. Spectrosc. Radiat. Transfer.*, **88**, 267 (2004).
- [12] Y. Shkuratov, S. Bondarenko, A. Ovcharenko, C. Pieters, T. Hiroi, H. Volten, O. Munos, G. Videen. *J. Quant. Spectrosc. Radiat. Transfer.*, **100**, 340 (2006).
- [13] E.V. Petrova, V.P. Tishkovets, K. Jockers. *Icarus*, **188**, 233 (2007).
- [14] M.I. Mishchenko, J.M. Dlugach, Li Liu. *Phys. Rev. A*, **80**, 053824 (2009).
- [15] M. Mishchenko, J. Dlugach, L. Liu, V. Rosenbush, N. Kiselev, Y. Shkuratov. *Astrophys. J. Lett.*, **705**, L118 (2009).
- [16] E. Zubko, Y. Shkuratov, M. Mishchenko, G. Videen. *J. Quant. Spectrosc. Radiat. Transfer.*, **109**, 2195 (2009).
- [17] E. Zubko, G. Videen, D.C. Hines, Yu. Shkuratov. In: 7 Moscow Intern. Solar System Symp. (7M-S3, IKI M., 2016), p. 124.
- [18] E. Zubko, A.J. Weinberger, N. Zubko. *Opt. Lett.*, **42**, 1962 (2017).
- [19] G. Videen, K. Muinonen. *J. Quant. Spectrosc. & Radiat. Transfer*, **150**, 87 (2015).
- [20] E. Zubko, D. Petrov, Y. Grynko, Y. Shkuratov, H. Okamoto, K. Muinonen, T. Nousiainen, H. Kimura, T. Yamamoto, G. Videen. *Appl. Opt.*, **49**, 1267 (2010).
- [21] W.B. Sun, G. Videen, Q. Fu, Y.X. Hu. *J. Quant. Spectrosc. Radiat. Transfer*, **131**, 166 (2013).
- [22] H. Lindqvist, J. Martikainen, J. Rabinäb, A. Penttiläb, K. Muinonen. *J. Quant. Spectrosc. & Radiat. Transfer*, **217**, 329 (2018).
- [23] A. Penttilä, T. Vaisanen, J. Markkanen, J. Martikainen, T. Kohout, G. Videen, K. Muinonen. *Icarus*, **345**, 113727 (2020). DOI: 10.1016/j.icarus.2020.113727
- [24] E.V. Petrova, V.P. Tishkovets, R.M. Nelson, M.D. Borita. *Astr. Vestnik*, **53** (3), 185 (2019) (in Russian).
- [25] Y. Shkuratov, D. Stankevich, D. Petrov, P. Pinet, A. Cord, Y. Daydou, S. Chevrel. *Icarus*, **173**, 3 (2005).
- [26] E.V. Klass. *Opt. Spectrosc.*, **123** (6), 983 (2017). DOI: 10.1134/S0030400X1711011X
- [27] E.V. Klass. *Opt. Spectrosc.*, **123** (6), 977 (2017). DOI: 10.1134/S0030400X17110121
A.M. Kolchuzhkin, V.V. Uchaikin. *Vvedeniye v teoriyu prokhozhdeniya chastits cherez veshchestvo* (Atomizdat, M., 1978) (in Russian).
- [29] S.M. Prigagin. *Osnovy statisticheskogo modelirovaniya perenosa polyarizovannogo opticheskogo izlucheniya: uchebnoe posobie* (Publishing house Novos. state university, Novosibirsk, 2010) (in Russian).
- [30] V.S. Degtyarev, L.O. Kolokolova. *Kinematika i fizika nebes. tel* **8** (2), 8 (1992) (in Russian).
- [31] E.V. Klass, V.V. Shakhovskii, K.V. Badyuk, S.A. Ulyanov. *Opt. zhurn.* **82** (2), 3 (2014) (in Russian).
- [32] E.V. Klass, S.A. Ulyanov. *Trudy 21-y Mezhdunar. konf. po komp'yut. grafike i zreniyu* (Graphicon-2011, Moscow, 2011) (in Russian).
- [33] L.M. Hanssen, A.V. Prokhorov. *Proc. SPIE.*, **7065**, 70650W-1 (2008).
- [34] B.G. Carlson. *Nucl. Scie. and Eng.*, **61**, 408 (1976).
- [35] Y. Grynko, Y. Shkuratov. *J. Quant. Spectr. & Radiat. Transfer*, **106**, 56 (2007).
- [36] J.-C. Worms, J.-B. Renard, A.C. Levasseur-Regourd, E. Hadamcik. *Adv. Space Res.*, **23** (7), 1257 (1999).
- [37] D.V. Sivukhin. *Obshchiy kurs fiziki. V. IV. Optika* (M., 1980) (in Russian).
- [38] *Osnovy optiki. Lecture notes*, ed. by A.A. Shekhonin (St. Petersburg State University ITMO, St. Petersburg, 2009) (in Russian).